Supplemental Material

Redescribing the response of yeast (*Saccharomyces cerevisiae*) to desiccation and rehydration

Jatinder Singh*§, Deept Kumar†, Naren Ramakrishnan†, Vibha Singhal†, Jody Jervis*, Steve Slaughter*, Andrea DeSantis*, Jamie Garst*, Malcolm Potts* and Richard F. Helm*¶

*Virginia Tech Center for Genomics, Fralin Biotechnology Center; †Department of Computer Science, Virginia Tech, Blacksburg, VA 24061

¶To whom correspondence should be addressed. E-mail: helmrf@vt.edu

§Present address: Department of Biomedical Sciences and Pathobiology, Virginia Tech, Blacksburg, VA 24061

Table of Contents

Materials and Methods.

Yeast Strains and Growth Conditions. The wild type strain *S. cerevisiae* BY4743 (*MATa*/*MAT*α *his3Δ1/hisΔ1 leu2δ0/leu2Δ0 lys2Δ0/+ met15Δ0/+ ura3Δ0/ura3Δ0*) was obtained from the ATCC. Stock and seed cultures were grown in yeast extract-peptone-dextrose (YPD) medium (10 mg/ml yeast extract, 20 mg/ml bactopeptone, 20 mg/ml glucose, pH 6.5 ± 0.2), at 30 °C. Cultures were shaken at 150 rpm and growth was monitored by measuring their absorbance at 600nm.

Cells were grown from a frozen stock culture of 200 µl which was added to 50 ml of YPD medium in a 500-ml Erlenmeyer flask, and incubated at 30 °C until cells reached the stationary phase of growth. A 6.25-ml aliquot of the cell suspension was used to inoculate 250 ml of YPD medium and the culture was incubated at 30 °C until the A_{600} reached 0.8. Cells were centrifuged at 3220 x g for 5 min. The supernatant fraction was discarded and the cell pellet was centrifuged once again and any residual liquid was removed using a gel-loading tip. The cells were resuspended and dispersed in 140 ml of 1:20 diluted YPD medium at between 22 to 25 °C. Different aliquots were removed for RNA extraction (5 ml), protein extraction (5 ml), carbohydrate analyses (2 ml), fluorescence activated cell sorting (FACS) analysis (2 ml), and viable counts (100 µl). Aliquots of 15 ml were dispensed into 9-cm diameter glass Petri dishes for desiccation. The experimental procedures were completed in three independent trials under conditions that were, as far as possible, identical.

Experimental Design Considerations. Microorganisms such as yeast are exposed to a wide variety of simultaneous stresses in natural settings, many of which lead to a substantial loss in viability. To mimic this phenomenon in the laboratory, a series of preliminary experiments were performed where the growth stage of the cells, the strength of the YPD medium, and the total time to complete dryness were treated as variables. A medium of YPD at a 1:20 dilution was chosen, as more concentrated YPD solutions were complicated by the formation of viscous solutions during desiccation (due to the hygroscopic nature of the media), whereas use of lower concentrations of YPD lead to more significant losses in cell viability. Drying times faster than 18h in 1/20 YPD led to a much higher mortality rate, whereas there was no advantage or disadvantage in allowing the desiccation process to take longer. Cells in the stationary phase of growth tended to show greater resistance to desiccation than cells in the logarithmic phase of growth. The cells were rehydrated in the same strength media (*ie*., 1/20 YPD), in an attempt to minimize glucose induced gene expression during rehydration, which could potentially mask the rehydration response.

Desiccation of Cells. Desiccation was carried out in a custom-fabricated Controlled Atmosphere Culture Desiccation System (CACDS), at 22 to 25 °C, where matric water potential (ψ) was controlled via a psychrometer sensor and computer controller. The CACDS modular component is a 24"x25"x24" (WxDxH) stock clean room storage enclosure (Terra Universal™, Irvine, CA) containing 2 individual closed atmosphere compartments. Continuous replenishment of low humidity atmosphere is provided by the NitroPlex™ Nitrogen atmosphere controller supplied with pre-purified nitrogen. The system has been retrofitted on-site to add a closed loop gas handling system, external gas conditioning chambers, environmental sensors, and computerized controller with custom software. The closed loop gas handling system is driven by two 2.5 CFM forced draft fans and is designed with a gas equalization manifold to provide for equalized gas flow and moisture exchange across samples. The system is also set up to allow recirculation of nitrogen atmosphere through modular external chambers containing desiccants or humidifying agents. An Airgas dual cylinder regulator was added to allow for the connection of two nitrogen cylinders for longer duration experiments. Computer controlled humidity and temperature sensors (PicoTechnology, St. Neots, UK) were added to refine environmental control parameters to a precision of 0.01% relative humidity and accuracy of +/- 2% relative humidity. Software developed on site provides the ability to monitor, control, graph and log environmental parameters within the chamber according to user specifications and experimental conditions. The latest version of the software provides the capability to also act as data logger capturing data from instruments inside the chamber as well as the ability to control three pinch valves (Takasago, Nagoya, Japan) added for switching between external desiccation,


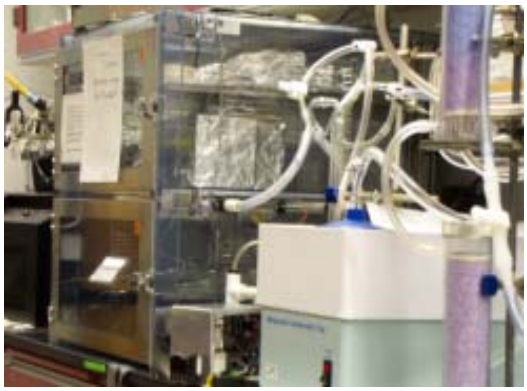

Figure S1. *Right*: Desiccator apparatus showing the water traps. *Left*: Nitrogen supply.

humidification, and recirculation systems. The computer is connected to the system through a custom electrical relay controller box which acts as a switch controller and data transfer controller to all integrated systems. For more information on the unit and software, contact Steve Slaughter, sslaugh@vt.edu.

Compressed nitrogen gas was circulated through a baffle system to achieve uniform drying within the chamber. Drying of cells was carried out at ψ = -163 MPa , where ψ = 1065. T. $\log_{10} p/p_o$; where T = °K, and p/p_o = water activity (a_w) that is numerically equivalent to relative humidity/100 (1). The relative humidity set point in this system was 30% ± 2. A second series of aliquots were withdrawn from the cell suspensions 18h (T_2) after the start of the drying process. Samples were collected on volume basis and were in the same ratio as collected at time T_1. Once dry (42 hr; T_{Dry}; 0.05 g residual H_20/g of cell solids), the water potential was adjusted to -218 MPa (20% relative humidity) for a period of 72 hr.

Hydration protocol/Cell Viability. Dry cells were hydrated (22 to 25 °C) using 1:20 diluted YPD medium, 15 ml per plate Cells were resuspended by gently rotating the plates in a circular motion, if needed, cells attached to the Petri dish were released by gentle repeat pipetting. Resuspended cells from the four plates were pooled in a sterile 250 ml flask. Samples were collected for various analyses at time points of 15 min (T_4), 45 min (T_5), 90 min (T_6) and 360 min (T_7) after the start of rehydration. Aliquots of 100µl were spread evenly on YPD agar (1.5% w/v) plates and plates were incubated at 30°C, for a period of 48 h, before counting colonies. Viability was assessed through serial dilution (10^{-1} to 10^{-5}) of cultures in sterile normal saline (0.85% sodium chloride, pH 7.2), at 22 to 25 °C. The remaining cells were spun down and flash frozen in liquid nitrogen, and stored at -70 °C until further use.

Extraction of RNA. Total RNA was isolated by the procedure of (2) modified as follows. Cells (in 5-ml aliquots) were harvested by centrifugation and resuspended in 800 µl of AE buffer (50 mM sodium acetate, 10 mM EDTA, pH 5.3,) and transferred to a 2.0-ml bead beater tube. Glass beads (total of 200 µl; each 0.5 mm in diameter), 80 µl of 10% w/v SDS and an equal volume of phenol (equilibrated in AE buffer) were added and the cells were homogenized at 4°C for 1 min, using the bead beater. Tubes were incubated at 65°C for 5 minutes and then chilled rapidly in dry ice/ethanol until phenol crystals appeared. At this point the mixture was centrifuged at room temperature, for 2 min. The aqueous phase was transferred to a new tube, an equal volume of phenol:chloroform (1:1 v/v; the latter containing iso-amyl alcohol at 24:1 v/v) was added, the contents were vortexed, and spun for 5 min at room temperature in a tube containing phase lock gel (Phase Lock Gel Heavy, Eppendorf). This step was repeated two times. The aqueous phase was extracted once with an equal volume of 100% chloroform. The aqueous phase was then transferred to a new tube, 1/10 volume of 3M sodium acetate, pH 5.3 and 2.5 volumes of ice-cold 100% ethanol were added, the contents were mixed, and nucleic acids were allowed to precipitate for 20 minutes, at -20°C. RNA was recovered through centrifugation and washed with 80% v/v ethanol. The RNA pellet was air dried and resuspended in 100 µl of diethyl pyrocarbonate-(DEPC) treated water. RNA was quantified using a spectrophotometer, and its quality was assessed using the A_{260}/A_{280} ratio.

Gene Expression Analyses. Three independent replicate microarray experiments, with seven sampling time points in each, and three replicates per time point, required 63 chips for hybridization analy-

sis. Analyses were performed at the University of Rochester Functional Genomics Center. Detailed protocols for sample preparation using the Affymetrix labeling protocols can be found at http://www.affymetrix.com. All samples were subjected to gene expression analysis via the Affymetrix Yeast S98 (single chip for whole genome) high-density oligonucleotide array probes.

Data Processing. Probe set signals were processed by a Wilcoxon's signed rank test (with significance thresholds of α_1=0.04 and α_2=0.06) to obtain detection calls of presence, absence, or marginal call. The pre-antibody amplification scan results (absolute signal values) were used only for those probe sets whose detection calls were present in the pre-antibody scan, but flagged as marginal or absent in the post-antibody scan. For all other probe sets, signal values were taken from the post-antibody amplification scan. A two-step linear mixed model was utilized to consolidate the nine measured signal values for each probe set. The normalization step calculates a residual using:

$$\log(\text{signal}) = \mu + T + S + TS + \text{residual}$$

where T is the treatment or time effect, and is fixed. The sample (S) and sample-treatment (TS) effects are modeled as random (the array effect could not be estimated independently since it was confounded with sample and treatment effects). The residual from the first step is modeled further as:

$$\text{residual} = P + PT + PS + \text{error}$$

where P is the probe set effect, and is fixed. The probe set-treatment (PT) effect is also fixed, being the value of interest. The probe set-sample effect (PS) was modeled as random. A very conservative Bonferroni adjustment of significance level 0.01 dictates an admissible -log(p- value) of –log(0.01/9335)=5.97 (where 9335 corresponds to the number of probe sets in the analysis). Relative expression estimates were derived with respect to both time point 1 (six comparisons) and time point 3, the onset of rehydration (four comparisons). A query-based website is available for accessing the microarray data (https://bioinformatics.cs.vt.edu/~vsinghal/yeast).

Preliminary Data Analysis. The Genesis Expression Similarity Investigation Suite (4), the TimeSearcher software from the University of Maryland, College Park (5), and machine learning techniques (6) such as inductive logic programming (ILP) (7) were utilized for a preliminary characterization of the global transcriptional response. The k-means clustering algorithm of Genesis was employed to identify dominant temporal patterns of gene expression. TimeSearcher allows the searching of gene expression data by temporal profiles, supporting interactive exploration of the dataset. Finally, for each comparison, the transcriptome was bucketed into gene subsets of the form:

$$\text{“expression} \in [a,b]\text{”}$$

and mapped into GO categories (biological, cellular, and molecular) using an ILP algorithm. The algorithm uses simultaneous covering and employs AD-trees (8) for fast counting purposes. The outputs of the algorithm are relational implications (one-directional rules, not redescriptions) from GO membership into gene subsets. The rules were post-processed for high confidence (0.8 and above) or for relating specific categories of interest, especially among very high or low expressors. The rules are presented as tile diagrams depicting category membership for various expression levels (see https://bioinformatics.cs.vt.edu/~vsinghal/yeast).

Design of Descriptors. We employed 11 types of vocabularies for descriptors that provide a total of just over 5000 descriptors (Table S1). All categories in the three parallel GO taxonomies applicable to *S. cerevisiae* were used to form descriptors based on functional and structural classifications. Expression levels from the comparisons presented here as well as published online experimental data were bucketed to yield range descriptors of the type "expression level is x and above", "expression level is x and below." K-

means clustering was applied to the high-expressors list for 20 and 10 cluster settings, for all comparisons with respect to time points 1 and 3, yielding 60 descriptors. The hydropathy index descriptors were based on predictive models of the tendency of an amino acid to be structurally inside the protein. Finally, expression buckets of data from a commercial dry active yeast was used to form a final class of descriptors.

Redescription Mining Algorithm. The goal of the algorithm is to learn equivalence relationships between set-theoretic expressions (involving union, intersection, and difference) defined on the space of descriptors. Redescriptions were mined using an alternating algorithm where decision trees were used as representations of set-theoretic expressions. In each iteration, the algorithm is given a decision tree as input and aims to grow (learn) another tree to match the set-expressions defined by the former; this new tree is then used as input for the next iteration. Thus, at any point, the trees are matched at possibly some (or all) of their leaves.

A training dataset is created in the following manner. The set of available descriptors D is first partitioned into two disjoint groups D_1 and D_2. For each gene, the (boolean) features are provided by membership in the D_1 descriptors and the classes are drawn from the D_2 descriptors. A greedy set-covering algorithm is employed to find a covering of the genes using D_2's sets; the selected sets from D_2 form the class labels. The decision tree is typically grown using entropy as the driving criterion, with possible randomized moves at the root level. This is to prevent over-dominance of one descriptor in the ensuing redescriptions. A pre-specified depth limit (often, 2) is imposed, for ease of interpretation. Class labels from D_2 are assigned to the leaves (e.g., the label that most reduces entropy), taking care that the same label is not assigned to all leaves. This is to maintain impurity and allow sufficient exploratory behavior on the part of the algorithm. Paths in the resulting tree are now "read off" as potential redescriptions and subject to evaluation by Jaccard's coefficient; this gives the strength of the redescription and is the ratio of genes that conform to it, to those that participate in either of the descriptors (but not necessarily in both). In this work, we used a Jaccard's threshold of 0.5. When reading off the boolean expressions, a conjunction (intersection) results from a path of length > 1 and a disjunction (union) results from multiple paths leading to the same class, with negations (set differences) corresponding to following the "no" branch from a given node.

The boolean expressions are then used to form class descriptors for the genes in the next iteration (hence, these classes are now descriptors derived from D_1, and can be complicated set-expressions). Note that these classes will be mutually exclusive and collectively exhaustive. All original D_2 descriptors now form the features (and are hence, simpler expressions). The process of learning the decision tree and reading of redescriptions is repeated. In the third iteration, classes are set-theoretic expressions formed using D_2's descriptors and features are taken directly from D_1, and so on. This "CARTwheels" algorithm is terminated when a certain desired number of redescriptions have been mined or when a given coverage of the underlying set has been obtained.

Within this basic framework, several implementation configurations are available. For our studies, we used an AD-tree for fast counting purposes and estimation of entropy. Tabular minimization is used for simplifying the boolean expressions read from trees. Syntactic constraints on redescriptions are incorporated as biases into the tree construction procedure. One example of a bias is a pre-specified requirement to preferentially look for patterns connecting past experimental results. Another example is to exclude redescriptions involving only NOTs for reasons mentioned below.

Formal analysis of the algorithm involves relating strategies for maintaining algorithmic exploration (*i.e.*, via randomization) to redescription quality metrics such as coverage. In addition, there is an intrinsic limit to a dataset's capability to reveal redescriptions, which can be studied through statistical analysis of set size distributions and estimates of overlap potential. Discussion of these is beyond the scope of this paper. Specialized redescription algorithms can also be designed for targeted descriptor families, *e.g.*, hierarchies.

Redescription results are presentable as equivalence relationships between descriptors (or combina-

tions of them), or *niches*. For example, redescription R5 (Fig, 4, main text; Fig. S5, Supplement) is as follows (with a Jaccard's coefficient of 0.71):

GASCH_ENV_11005 × exc-DESIC_GRE _1_2_0001 and DESIC_GRE _1_2_00013

In a modified form the statement is read as follows:

Heat shock 30 min - -1 × T_2 *vs.* T_1 • -5 AND NOT T_2 *vs.* T_1 • -1

This redescription, automatically mined by the algorithm, relates descriptors between a vocabulary based on our desiccation expression levels (DESIC) and one based on published expression levels of Gasch *et al.* (GASCH) (3). The redescription is read as: "Among the 210 high-expressors, the only genes that are 1-fold or more down-regulated in the Heat shock 30 minutes time point are also those genes that are between 1-fold and 5-fold down-regulated in desiccation time point 2." 32 genes conform to this redescription, meaning they can equally well be described by either the expression on the left or the one on the right. 35 genes participate in the left descriptor and 42 genes participate in the right descriptor, with 32 common, thus yielding 32/(35 + 42 – 32) = 0.71 as the Jaccard's coefficient. More redescriptions can be found in Fig. S5.

Notice that the redescription algorithm has automatically created a restriction (difference) on the right, in order to create two set expressions that more or less refer to the same members. Neither the members of the set, nor the ways in which the descriptors must be combined are instructed to the algorithm – only the underlying vocabularies are provided from which the descriptors are drawn. The algorithm internally searches through myriad combinations of creating set expressions that overlap significantly. For instance, consider the redescription

GASCH_ENV_11005 × DESIC_GRE_1_2_00013

in other words – "The only genes that are 1-fold or more down regulated in the Heat shock 30 minutes time point are also those genes that are 1-fold or more down-regulated in desiccation time point 2". 35 genes participate in the left descriptor, 76 genes participate in the right, yielding a poor Jaccard's score of 35/(35 + 76 – 32), or only 0.44. There are thus too many genes on the right with not enough in common with the left. To arrive at a better redescription, the algorithm has automatically restricted the scope of the right side to exclude some genes.

Interpreting Redescriptions: It is important to note that the descriptors underlying a mined redescription refer to a set of genes, in the context of a larger universal set (here, the 210 high-expressors). Hence, all redescriptions must be interpreted carefully in the context of this larger set. Thus, when we use "genes that are between 1-fold and 5-fold down regulated in desiccation time point 2", this descriptor defines the 42 genes only when applied within the high-expressors. If the entire set of yeast ORFs is included, these descriptors now acquire different meanings, and the redescription may or may not hold.

Another consideration while assessing redescriptions is as follows. Since redescriptions are equivalence relationships, a set-expression such as A × B also means that (NOT A) × (NOT B); in other words redescriptions occur in pairs. However, when using the Jaccard's coefficient as a measure of redescription quality, we must be careful to explicitly check and see if the inverse of a mined redescription also holds. This is because a redescription may happen by chance if both the left and right sides cover more than, say, 80% of the universal set. As a concrete example, the redescription

NOT DESIC_GRE_1_7_00005 × NOT KMC_TRENDS_1_20_14

holds with Jaccard's coefficient (118 / (205 + 118 – 118)) = 0.58, but is not immediately useful as a biologi-

cal result due to the negations in the descriptors. In fact, the left side is a proper subset of the right. Restating it as

$$\text{DESIC\_GRE\_1\_7\_00005} \times \text{KMC\_TRENDS\_1\_20\_14}$$

does not yield the expected results, since the Jaccard's coefficient drops to (5 / (5 + 92 - 5)) = 0.054 (notice now that the right descriptor is a subset of the left). *Another way of saying this is that it is safe to invert a redescription that holds with Jaccard's coefficient equal to 1 but not necessarily others.*

Plans are currently being made to release the CARTwheels implementation in the public domain. For more details, contact Naren Ramakrishnan (naren@cs.vt.edu)

Protein Isolation. Yeast whole cell extracts were prepared as described by (9) modified as follows. Cells were collected by centrifugation and washed in 5 ml cold extraction buffer (200 mM Tris, 150 mM ammonium sulfate, 10% v/v glycerol, 1 mM EDTA, pH 8.0), containing 2 mM DTT and protease inhibitors (1.0 mM phenylmethylsulfonylfluoride, 2.0 mM benzamidine, 0.6 µM leupeptin, 2.0 µM pepstatin and 10 µM chymostatin). The following procedures were all performed at 4 °C. Cells were resuspended in 600 µl of extraction buffer then transferred to a 2-ml bead beater tube on ice. Glass beads (200 µl) were added to the tube and the cells were homogenized for 1 minute. The tubes were kept on ice for at least 1 min in between homogenizations in the bead beater. The process was repeated five times. Cell debris was removed by centrifugation. The supernatant fraction was transferred to a microcentrifuge tube, leaving most of the glass beads behind, and centrifuged at 20,800 x g, for 30 min. The supernatant fraction was recovered and protein concentration was measured using Coomassie protein assay reagent (Pierce) according to the manufacturer's directions.

Carbohydrate Analysis. Cells were collected from 1 ml aliquots by centrifugation at 20,800 x g for 5 min and stored at -70 °C until further use. The cell pellet was washed by resuspension in 1 ml ice-cold water, vortexed, and stored on ice for 10 min. Cells were collected by centrifugation at 20,800 x g for 5 min. Washed cells were resuspended in 250µl of ice-cold water and transferred to a 2-ml bead beater tube to which 200µl of acid washed, 0.5-mm glass beads (BioSpec Products, Inc.) were added. Cell lysates were prepared in the bead beater using 5 rounds of 60 s duration. The tubes were stored on ice in between rounds of shaking. Cell debris was removed by centrifugation at 20,800 x g for 30 min. The supernatant fraction was transferred to a new 1.5-ml tube and further clarified by a second round of centrifugation. The clarified lysate was transferred to a new tube, flash-frozen and freeze dried.

Freeze dried cell lysate was dissolved in 200µl of HPLC grade water and passed over a 1-ml Strata C18-E solid phase column washed previously with one column volume of methanol followed by one column volume of HPLC grade water. Carbohydrates were eluted from the column using two column volumes of HPLC grade water. The eluate was flash-frozen, freeze dried and dissolved in 200µl of HPLC grade water and analyzed as follows.

Carbohydrate analysis was performed using high pressure anion exchange-pulsed amperometric detection (HPAE-PAD). The chromatography system (Dionex) consisted of a GP50 gradient pump, an ED50 electrochemical detector, and an LC 50 column oven. Mobile phases (Eluant A = HPLC grade water, Eluant B and C = 100mM NaOH, Eluant D = 100mM NaOH in 1 M sodium acetate) were installed on the chromatography system and pressured with nitrogen (6 psi). Standards and samples (20 µl injections) were separated with a CarboPac PA 10 column set (0.4 x 25cm + guard, Dionex). The flow rate was 1.0ml/min and the column was maintained at 30 °C. The gradient was 80mM NaOH for 15 minutes, followed by a five minute gradient to a five minute 500 mM sodium acetate wash then returning to 15 min equilibrium at starting conditions. Carbohydrates were detected by pulsed amperometry using the following pulsed amperometric waveforms (0s, 0.1v), (0.2s, 0.1v), (0.4s, 0.1v), (0.41s, -2.0v), (0.42s, -2.0v), (0.43s, 0.6v),

(0.44s, -0.1v), and (0.5s, -0.1v). The current was integrated between 0.2s and 0.4s and the data were collected at the frequency of 2 Hz.

Flow Cytometry. Cell cycle analysis followed the procedure of (10) modified as follows. Cells were harvested by centrifugation at 3220 x g, for 5 minutes, and pellets were resuspended in 1.5 ml sterile water, followed by the addition of 3.5 ml of 95% v/v ethanol. The fixed cells were stored at 4 °C until further use. For staining, a 500-µl aliquot of the suspension was centrifuged and the recovered pellet was resuspended first in 1 ml of water, and after centrifugation, in 0.5 ml of 50 mM Tris-HCl, pH 8.0. RNase A (10 µl of 10mg/ml) was added and the cells were incubated for 4 hr at 37 °C, and then kept overnight at 4 °C. The cells were recovered by centrifugation and resuspended in 0.5 ml 50 mM Tris-HCl, pH 7.5, containing 2mg/ml proteinase K, and incubated at 50 °C for 30 minutes. The cells were then recovered and resuspended in 0.5 ml of FACS buffer (200 mM Tris-HCl, 200 mM NaCl, 78 mM $MgCl_2$, pH 7.5). A 100-µl aliquot was transferred to a new tube and 1 ml of 1x Sytox Green (Molecular Probes, Eugene, OR; S-7020) solution in 50 mM Tris-HCl pH 7.5, was added, with a final concentration of the stain of 1 µM. The cells were analyzed using a flow cytometer (Beckman Coulter, EPICS-XL). Software used for data analysis was EPICS version 1.5.

Measurement of Cell Water Content. Intracellular water content was determined by thermogravimetric analysis as outlined (11) with the following modifications. Desiccated cells were harvested by scraping them from the surface of the glass Petri dishes using a surgical blade. The powder was transferred to a 10-mm diameter platinum pan and analysis was conducted with a TA-Instruments Hi-Res. TGA 2950 thermogravimetric analyzer. Starting from room temperature, with a heating rate of 10 C°/min, the temperature was raised to 60 °C. When the mass loss rate was practically zero, the temperature was raised to 125 °C for 7 min in order to complete the water elimination and to determine the water-free residual mass.

Protein analyses. Yeast whole cell extracts were separated on 12% SDS-PAGE gels and stained with either Coomassie (Brilliant Blue R 250,), SYPRO-Ruby, or Pro-Q Diamond gel stains (Molecular Probes) according to the directions of the manufacturer. Protein bands of interest were excised using a gel-coring tool, and the excised gel pieces were placed in a 0.5ml siliconized tube (VWR). A 100-µl solution of 25mM NH_4HCO_3/ 50% acetonitrile was added and the tubes were vortexed, overnight. After destaining, the gel pieces were dehydrated using 100% acetonitrile (100 µl). Once the gel pieces turned opaque-white in color, acetonitrile was removed and the gel pieces were allowed to air dry for 3-5 min.

A 30µl aliquot of 10mM dithiothreitol (DTT) solution was added to the gel pieces and incubated for 30-45 min at 37 °C. The DTT solution was replaced with 100µl of 55mM iodoacetamide and tubes were incubated at 56 °C for 45 min. At the end of the incubation period, the gel pieces were washed with 100µl of 25mM NH_4HCO_3 pH 8.0, for 10 min while vortexing at a low speed. The gel pieces were dehydrated using 100% acetonitrile until they turned opaque-white color.

Gel pieces were hydrated on ice for 10-15 min, in 25 µl of trypsin solution. Excess trypsin solution was removed and the gel pieces were overlayed with 30 µl of 25 mM NH_4HCO_3, and incubated for a period of 12-16 h. A 5µl volume of 5% trifluroacetic acid solution (TFA) was added to the tubes, to halt the process of digestion. The tubes were vortexed for 10 min and then centrifuged briefly, and stored at -20 °C until further use.

Digested protein samples were analyzed on an LC-tandem mass spectrometer (LC Packings HPLC and a Thermo-Finnigan LCQ-Deca-XP fitted with a nanospray source. A fused silica capillary of 75 µm inner diameter was packed in-house to 5 cm with C_{18} material (Phenomenex, Jupiter 4 µm, 90 A). A 4 µl aliquot of the protein digest was injected on the column using a pressure bomb at 500psi. A gradient of 0.5% HOAc:MeCN was used, the gradient being 95:5 at the start of the run (T_0) and 25:75 at the end of the run (T_{43min}), at a flow rate of 110 nl/min. A full data dependent scan with the m/z range of 300-2000 was used. Data were analyzed with SEQUEST using the protein database (indexed for speed) available from NCBI.

References

1. Potts, M., Friedmann, E. I. (1981) *Arch. Microbiol.* **130**, 267-271.
2. Schmitt, M. E., Brown, T. A. , Trumpower, B. L. (1990) *Nucl. Acids Res.* **18,** 3091-3092.
3. Gasch, A. P., Spellman, P. T., Kao, C. M., Carmel-Harel, O., Eisen, M. B., Storz, G., Botstein, D. Brown, P. O. (2000) *Molec. Biol. Cell* **11,** 4241-4257.
4. Sturn, A., Quackenbush, J., Trajanoski, Z. (2002) *Bioinformatics* **18**, 207-208.
5. Hochheiser, H., Shneiderman, B. (2001) in *Lecture Notes in Computer Science*, Vol. 2226, eds. Klaus, P. J. & Ayuma, S. (Springer, Heidelberg), pp. 441-446.
6. Molla, M., Waddell, M., Page, D., Shavlik, J. (2004) *Artif. Intell. Mag*.,to appear.
7. Muggleton, S. (1999) *Commun. ACM* **42**, 42-46.
8. Moore, A., Lee, M.S. (1998) *J. Artif. Intell. Res.* **8**, 67-91.
9. Auble, D. T., Wang, D. Y., Post, K. W., Hahn, S. (1997) *Mol. Cell. Biol.* **17,** 4842-4851.
10. MacKay, V. L., Mai, B., Waters, L., Breeden, L. L. (2001) *Mol. Cell. Biol.* **21,** 4140-4148.
11. Alcazar, E. B., Rocha-Leao, M. H. M. , Dweck, J. (2000) *J. Thermal Anal. Calorim.* **59,** 643-648.

Table S1. Descriptor vocabularies and domains.

Vocabulary	Domain	Number of Descriptors	Source[1]
GO_CEL	GO Cellular Component Category	336	SGD
GO_BIO	GO Biological Process Category	1404	SGD
GO_MOL	GO Molecular Function Category	1494	SGD
DESIC	Expression levels: this work	303	this work
GASCH	Expression levels: Gasch *et al.*	936	A
HISTONE	Expression levels: Histone depletion	231	B
KMC	k-means clusters (from DESIC)	60	this work
HYDRO_INDEX	Hydropathic protein index	33	C
HYDRO_SCORE	Hydropathic protein score	37	C
MOD_HYDRO_INDEX	Modified protein hydropathicity	39	C
DRY_ACTIVE	Expression level: commercial yeast	32	this work

[1]SGD, Saccharomyces genome database

A Gasch AP, Spellman PT, Kao CM, Carmel-Harel O, Eisen MB, Storz G, Botstein D, Brown PO (2000) Genomic expression programs in the response of yeast cells to environmental changes. *Mol. Biol. Cell* **11**: 4241-57.

B Wyrick JJ, Holstege FC, Jennings EG, Causton HC, Shore D, Grunstein M, Lander ES, Young RA (1999) Chromosomal landscape of nucleosome-dependent gene expression and silencing in yeast. *Nature* **402**: 418-21.

C Garay-Arroyo A, Colmenero-Flores JM, Garciarrubio A, Covarrubias AA. (2000) Highly hydrophilic proteins in prokaryotes and eukaryotes are common during conditions of water deficit. *J. Biol. Chem.* **275**: 5668-74.

Table S2. List of 210 "High Expressors" Used in the Redescriptions

Probe	Annotation
10026_at	YLR311C weak similarity to S.tarentolae cryptogene protein G4
10027_at	YLR312C hypothetical protein
10029_at	YLR314C Component of 10 nm filaments of mother-bud neck
10043_at	YLR284C Peroxisomal enoyl-CoA hydratase
10154_at	YLR174W Cytosolic form of NADP-dependent isocitrate dehydrogenase
10160_at	YLR180W S-adenosylmethionine synthetase
10300_f_at	YLR048W Ribosomal protein S0B
10473_i_at	YKR094C Ribosomal protein L40B
10478_at	YKR097W phosphoenolpyruvate carboxylkinase
10602_at	YKL050C similarity to YMR031c
10658_at	YKL081W Translation elongation factor EF-1gamma
10677_at	YKL107W weak similarity to S.antibioticus probable oxidoreductase
10705_g_at	YKL124W suppressor of SHR3; confers leflunomide resistance when overexpressed
10776_at	YKL187C strong similarity to hypothetical protein YLR413w
10795_at	YKL217W carboxylic acid transporter protein homolog
10800_at	YKL212W integral membrane protein localizing to the ER and Golgi
10934_at	YJR095W protein related to mitochondrial carriers
11068_at	YJL045W strong similarity to succinate dehydrogenase flavoprotein
11113_at	YJL089W shows homology to DNA binding domain of Gal4p, has a leucine zipper motif and acidic region; exA-Sip4p activates transcription
11114_at	YJL088W Ornithine carbamoyltransferase
11185_at	YJL153C L-myo-inositol-1-phosphate synthase
11203_i_at	YJL177W Ribosomal protein L17B (L20B) (YL17)
11297_at	YAR035W Outer carnitine acetyltransferase, mitochondrial
11355_at	YAL012W cystathionine gamma-lyase
11386_at	YAL062W NADP-linked glutamate dehydrogenase
2129_s_at	Saccharomyces cerevisiae chromosome VIII, complete chromosome sequence. Found forward in NC_001140 between 312647 and 313497 with 100% identity.
2162_g_at	Saccharomyces cerevisiae chromosome VII, complete chromosome sequence. Found forward in NC_001139 between 959166 and 960165 with 100% identity.
2163_s_at	Saccharomyces cerevisiae chromosome VII, complete chromosome sequence. Found forward in NC_001139 between 960166 and 960596 with 100% identity.
2182_s_at	Saccharomyces cerevisiae chromosome VII, complete chromosome sequence. Found forward in NC_001139 between 136050 and 137049 with 100% identity.
2183_s_at	Saccharomyces cerevisiae chromosome VII, complete chromosome sequence. Found forward in NC_001139 between 137050 and 138049 with 100% identity.
2259_at	Saccharomyces cerevisiae chromosome VII, complete chromosome sequence. Found forward in NC_001139 between 108045 and 109044 with 100% identity.
2260_g_at	Saccharomyces cerevisiae chromosome VII, complete chromosome sequence. Found forward in NC_001139 between 108045 and 109044 with 100% identity.
2261_s_at	Saccharomyces cerevisiae chromosome VII, complete chromosome sequence. Found forward in NC_001139 between 109045 and 109906 with 100% identity.
2280_s_at	Saccharomyces cerevisiae chromosome V, complete chromosome sequence. Found forward in NC_001137 between 112004 and 113003 with 100% identity.
2603_s_at	Saccharomyces cerevisiae chromosome XVI, complete chromosome sequence. Found forward in NC_001148 between 109147 and 110146 with 100% identity.
2835_at	Saccharomyces cerevisiae chromosome XII, complete chromosome sequence. Found forward in NC_001144 between 809817 and 810816 with 100% identity.
2836_g_at	Saccharomyces cerevisiae chromosome XII, complete chromosome sequence. Found forward in NC_001144 between 809817 and 810816 with 100% identity.
2837_s_at	Saccharomyces cerevisiae chromosome XII, complete chromosome sequence. Found forward in NC_001144 between 810817 and 811816 with 100% identity.
2838_s_at	Saccharomyces cerevisiae chromosome XII, complete chromosome sequence. Found forward in

	C_001144 between 811817 and 812816 with 100% identity.
2839_s_at	Saccharomyces cerevisiae chromosome XII, complete chromosome sequence. Found forward in NC_001144 between 812817 and 813816 with 100% identity.
3182_i_at	YHR217C strong similarity to subtelomeric encoded YDR544c
3243_at	TL(GAG)G tRNA-Leu
3371_f_at	TE(UUC)E1 tRNA-Glu
3437_f_at	TR(UCU)D tRNA-Arg
3482_f_at	TE(UUC)B tRNA-Glu
3491_f_at	TE(UUC)C tRNA-Glu
3545_i_at	YBLWDELTA1 Ty1 LTR
3546_f_at	YBLWDELTA1 Ty1 LTR
3594_f_at	TE(UUC)P tRNA-Glu
3680_i_at	YMRWDELTA15 Ty1 LTR
3687_f_at	TR(UCU)M1 tRNA-Arg
3709_f_at	TE(UUC)M tRNA-Glu
3758_f_at	TE(UUC)L tRNA-Glu
3764_s_at	RDN37-1 35S ribosomal RNA
3768_i_at	RDN5-1 5S ribosomal RNA
3813_f_at	TE(UUC)K tRNA-Glu
3838_s_at	TM(CAU)J3 tRNA-Met
3850_at	YJRWDELTA20 Ty1 LTR
3858_s_at	TN(GUU)K tRNA-Asn
3862_f_at	TR(UCU)J1 tRNA-Arg
3863_f_at	TR(UCU)J2 tRNA-Arg
3864_i_at	YJLCDELTA6 Ty1 LTR
3878_s_at	TL(UAA)J tRNA-Leu
3884_f_at	TE(UUC)J tRNA-Glu
3905_s_at	TD(GUC)J1 tRNA-Asp
3923_f_at	TA(UGC)A tRNA-Ala
3959_at	F1F0-ATPase complex, FO A subunit Found forward in NC_001224 between 28487 and 29266 with 97.564103% identity.
3975_at	ubiquinol—cytochrome-c reductase subunit (cytochrome B) Found forward in NC_001224 between 43297 and 43647 with 100% identity.
3977_i_at	similarity to honeybee mitochondrion NADH dehydrogenase chain 6 (SGC4) Found reverse in NC_001224 between 48858 and 49169 with 99.679487% identity.
3981_at	probable mRNA maturase in 21S rRNA intron Found forward in NC_001224 between 61193 and 61729 with 100% identity.
3985_i_at	questionable ORF Found forward in NC_001224 between 74495 and 74804 with 99.677419% identity.
3998_at	COX1 intron 1 protein Found forward in NC_001224 between 13818 and 16322 with 99.92016% identity.
4008_at	cytochrome-c oxidase subunit I Found forward in NC_001224 between 26627 and 26701 with 100% identity.
4160_at	YIL057C strong similarity to YER067w
4241_at	YIL160C peroxisomal 3-oxoacyl CoA thiolase
4365_at	YHR160C weak similarity to hypothetical protein YGR239c
4388_at	YHR139C sporulation-specific wall maturation protein
4428_at	YHR092C High-affinity glucose transporter
4432_at	YHR096C hexose transporter
4478_at	YHR049W similarity to S.pombe dihydrofolate reductase and YOR280c
4491_at	YHR063C weak similarity to translational activator CBS2
4507_at	YHR033W Pro1p (Gamma-glutamyl kinase)
4561_s_at	SNR7-L snRNA
4672_at	non-annotated SAGE orf Found forward in NC_001139 between 110756 and 110950 with 100% identity. See citation Velculescu, V.E., et al. (1997) Characterization of the yeast transcriptome. Cell 8:243-251
4686_s_at	non-annotated SAGE orf Found reverse in NC_001139 between 939417 and 939581 with 100%

	identity. See citation Velculescu, V.E., et al. (1997) Characterization of the yeast transcriptome. Cell 8:243-251
4754_at	YGR234W Flavohemoglobin
4756_at	YGR236C questionable ORF
4813_at	YGR203W weak similarity to X.laevis protein-tyrosin-phosphatase cdc homolog 2 and to hypothetical protein YPR200c
4884_i_at	YGR138C similarity to multidrug resistance proteins
4969_at	YGR043C strong similarity to transaldolase
5005_at	YGL012W Sterol C-24 reductase
5016_at	YGL001C putative 3-beta-hydroxysteroid dehydrogenase
5076_f_at	YGL076C Ribosomal protein L7A (L6A) (rp11) (YL8)
5177_at	YGL158W Serine/threonine protein kinase
5178_at	YGL157W similarity to V.vinifera dihydroflavonol 4-reductase
5220_at	YGL205W fatty-acyl coenzyme A oxidase
5310_at	YFR055W strong similarity to beta-cystathionases
5372_at	YFL014W 12 kDa heat shock protein
5413_at	RPR1 RNase P RNA
5416_at	SNR14 snRNA R14
5528_at	YER179W meiosis-specific protein related to RecA and Rad51p. Dmc1p colocalizes with Rad51p to discrete subnuclear sites in nuclear spreads during mid prophase, briefly colocalizes with Zip1p, and then disappears by pachytene
5550_at	YER156C similarity to hypothetical C. elegans protein C27H6.5
5571_at	YER131W Ribosomal protein S26B
5612_at	YER084W questionable ORF
5627_at	YER096W sporulation-specific homolog of csd4
5636_at	YER065C isocitrate lyase
5667_at	YER055C ATP phosphoribosyltransferase
5679_at	YER024W similarity to carnitine O-acetyltransferase Yat1p
5698_at	YER043C putative S-adenosyl-L-homocysteine hydrolase
5750_at	YEL040W weak similarity to Bacillus 1,3-1,4-beta-glucanase
5925_at	YDR524c-a identified by SAGE
5985_at	YDR471W Ribosomal protein L27B
6131_at	YDR345C High-affinity glucose transporter
6221_at	YDR256C catalase A
6234_at	YDR223W similarity to Ifh1p
6346_at	YDR111C strong similarity to alanine transaminase
6413_at	YDR044W Coproporphyrinogen III oxidase
6556_at	YDL085W strong similarity to NADH dehydrogenase (ubiquinone)
6558_i_at	YDL083C Ribosomal protein S16B (rp61R)
6560_at	YDL082W Ribosomal protein L13A
6612_at	YDL119C similarity to bovine Graves disease carrier protein
6665_at	YDL198C high copy suppressor of abf2 lacking the HMG1-like mitochondrial HM protein; putative mitochondrial carrier protein
6694_at	YDL214C strong similarity to putative protein kinase NPR1
6712_at	YDL241W hypothetical protein
6729_at	YDL223C weak similarity to mucin
6765_at	non-annotated SAGE orf Found forward in NC_001135 between 41465 and 41704 with 100% identity. See citation Velculescu, V.E., et al. (1997) Characterization of the yeast transcriptome. Cell 8:243-251
6887_at	YCR010C strong similarity to Y.lipolytica GPR1 protein and Fun34p
6951_at	TLC1 telomerase RNA component
6953_at	LSR1 snRNA
6968_at	non-annotated SAGE orf Found reverse in NC_001134 between 681184 and 681420 with 100% identity. See citation Velculescu, V.E., et al. (1997) Characterization of the yeast transcriptome. Cell 8:243-251
6980_at	non-annotated SAGE orf Found reverse in NC_001134 between 376102 and 376293 with 100% identity. See citation Velculescu, V.E., et al. (1997) Characterization of the yeast transcriptome.

	Cell 8:243-251
7103_at	YBR238C strong similarity to general chromatin factor Spt16p
7114_at	YBR249C 3-deoxy-D-arabino-heptulosonate 7-phosphate (DAHP) synthase isoenzyme
7190_i_at	YBR189W Ribosomal protein S9B (S13) (rp21) (YS11)
7253_g_at	YBR116C questionable ORF
7254_at	YBR117C transketolase, homologous to tkl1
7273_at	YBR092C Acid phosphatase, constitutive
7313_at	YBR045C Glc7-interacting protein.
7403_at	YBL049W hypothetical protein
7404_at	YBL048W hypothetical protein
7409_at	YBL043W ExtraCellular Mutant
7413_at	YBL039C CTP synthase, highly homologus to URA8 CTP synthase
7422_at	YBL075C heat-inducible cytosolic member of the 70 kDa heat shock protein family
7431_at	YBL065W questionable ORF
7477_at	SNR45 snRNA
7503_i_at	non-annotated SAGE orf Found reverse in NC_001148 between 880229 and 880366 with 100% identity. See citation Velculescu, V.E., et al. (1997) Characterization of the yeast transcriptome. Cell 8:243-251
7588_at	YPR145W asparagine synthetase
7594_at	YPR151C weak similarity to YPL159c
7694_at	YPR074C Transketolase 1
7714_at	YPR049C similarity to Uso1p
7753_at	YPR001W Mitochondrial isoform of citrate synthase
7754_at	YPR002W similarity to B.subtilis mmgE protein
7781_at	YPL017C strong similarity to Lpd1p and other dihydrolipoamide dehydrogenases
7810_at	YPL033C weak similarity to YLR426w
7811_at	YPL079W Ribosomal protein L21B
7854_i_at	YPL081W Ribosomal protein S9A (S13) (rp21) (YS11)
7923_at	YPL147W Pxa1p and Pxa2p appear to be subunits of a peroxisomal ATP-binding cassette transporter necessary for transport of long-chain fatty acids into peroxisomes
7957_at	YPL201C hypothetical protein
7960_i_at	YPL198W Ribosomal protein L7B (L6B) (rp11) (YL8)
7981_at	YPL223C Induced by osmotic stress
7993_at	YPL256C G(sub)1 cyclin
8020_s_at	YPL276W putative formate dehydrogenase/putative pseudogene
8067_i_at	non-annotated SAGE orf Found reverse in NC_001147 between 974085 and 974252 with 100% identity. See citation Velculescu, V.E., et al. (1997) Characterization of the yeast transcriptome. Cell 8:243-251
8142_s_at	YOR388C Protein with similarity to formate dehydrogenases
8192_at	YOR348C putative proline-specific permease
8228_at	YOR338W similarity to YAL034c
8246_s_at	YOR309C questionable ORF
8269_f_at	YOR293W Ribosomal protein S10A
8382_at	YOR180C Peroxisomal enoyl-CoA hydratase
8437_at	YOR100C similarity to mitochondrial carrier proteins
8504_at	YOR031W Metallothionein-like protein
8548_at	YOL014W hypothetical protein
8577_at	YOL030W strong similarity to glycoprotein Gas1p
8711_i_at	non-annotated SAGE orf Found reverse in NC_001146 between 651893 and 652045 with 100% identity. See citation Velculescu, V.E., et al. (1997) Characterization of the yeast transcriptome. Cell 8:243-251
8776_at	YNR064C similarity to R.capsulatus 1-chloroalkane halidohydrolase
8862_at	YNR014W weak similarity to hypothetical protein YMR206w
8881_at	YNL014W translation elongation factor eEF3 homolog
8886_at	YNL009W peroxisomal NADP-dependent isocitrate dehydrogenase
8922_at	YNL066W Protein involved in the aging process
8959_at	YNL117W carbon-catabolite sensitive malate synthase

9026_at	YNL142W Ammonia transport protein
9057_at	YNL202W peroxisomal 2,4-dienoyl-CoA reductase
9063_at	YNL196C sporulation-specific protein with a leucine zipper motif, regulated by the transcription factor Ume6 and expressed early in meiosis
9124_at	YNL270C Protein highly homologous to permeases Can1p and Lyp1p for basic amino acids
9196_s_at	YNL335W similarity to M.verrucaria cyanamide hydratase, identical to hypothetical protein YFL061w
9219_i_at	non-annotated SAGE orf Found forward in NC_001145 between 483361 and 483495 with 100% identity. See citation Velculescu, V.E., et al. (1997) Characterization of the yeast transcriptome. Cell 8:243-251
9220_r_at	non-annotated SAGE orf Found forward in NC_001145 between 483361 and 483495 with 100% identity. See citation Velculescu, V.E., et al. (1997) Characterization of the yeast transcriptome. Cell 8:243-251
9221_f_at	non-annotated SAGE orf Found forward in NC_001145 between 483361 and 483495 with 100% identity. See citation Velculescu, V.E., et al. (1997) Characterization of the yeast transcriptome. Cell 8:243-251
9223_at	non-annotated SAGE orf Found forward in NC_001145 between 611313 and 611507 with 100% identity. See citation Velculescu, V.E., et al. (1997) Characterization of the yeast transcriptome. Cell 8:243-251
9274_at	non-annotated SAGE orf Found reverse in NC_001145 between 29913 and 30104 with 100% identity. See citation Velculescu, V.E., et al. (1997) Characterization of the yeast transcriptome. Cell 8:243-251
9275_g_at	non-annotated SAGE orf Found reverse in NC_001145 between 29913 and 30104 with 100% identity. See citation Velculescu, V.E., et al. (1997) Characterization of the yeast transcriptome. Cell 8:243-251
9276_at	non-annotated SAGE orf Found reverse in NC_001145 between 30023 and 30229 with 100% identity. See citation Velculescu, V.E., et al. (1997) Characterization of the yeast transcriptome. Cell 8:243-251
9287_s_at	YMR322C strong similarity to YPL280w, YOR391c and YDR533c
9309_at	YMR303C alcohol dehydrogenase II
9390_at	YMR251W-A hyperosmolarity-responsive gene
9397_at	YMR215W similarity to GAS1 protein
9444_at	YMR174C Cytoplasmic inhibitor of proteinase Pep4p
9445_at	YMR175W protein of unknown function
9510_at	YMR114C similarity to B. subtilis conserved hypothetical proteins yoqW and yoaM
9515_at	YMR118C strong similarity to succinate dehydrogenase
9549_at	YMR107W hypothetical protein
9571_at	YMR085W putative pseudogene
9668_at	YML042W Carnitine O-acetyltransferase, peroxisomal and mitochondrial
9700_at	YML056C strong similarity to IMP dehydrogenases
9756_at	YML089C questionable ORF
9794_at	SNR6 snRNA
9795_at	SNR61 snRNA
9947_i_at	YLR367W Ribosomal protein S22B (S24B) (rp50) (YS22)
9958_at	YLR377C fructose-1,6-bisphosphatase
9964_at	YLR340W 60S ribosomal protein P0 (A0) (L10E)

Table S3. List of the genes up-regulated 4-fold or higher at the T_{Dry} timepoint.

Probe	Gene	SDC	Annotation	Fold Change
8142_s_at	YOR388C	FDH1	Formate dehydrogenase	8.4884
9445_at	YMR175W	SIP18	Protein of unknown function	8.3648
10677_at	YKL107W	YKL107W	Weak similarity to *S.antibioticus* probable oxidoreductase	7.5804
8020_s_at	YPL276W	FDH2	Formate dehydrogenase	7.3315
7422_at	YBL075C	SSA3	Heat-inducible cytosolic member of the 70 kDa heat shock protein family	7.3127
10934_at	YJR095W	SFC1	Protein related to mitochondrial carriers	7.2617
9515_at	YMR118C	YMR118C	Strong similarity to succinate dehydrogenase	6.6536
11068_at	YJL045W	YJL045W	Strong similarity to succinate dehydrogenase flavoprotein	6.6298
7981_at	YPL223C	GRE1	Induced by osmotic stress	6.4044
7957_at	YPL201C		Hypothetical protein	6.3418
8437_at	YOR100C	CRC1	Similarity to mitochondrial carrier proteins	6.331
5925_at	YDR524C-B		Hypothetical small protein	6.29
7753_at	YPR001W	CIT3	Mitochondrial isoform of citrate synthase	6.264
8959_at	YNL117W	MLS1	Carbon-catabolite sensitive malate synthase	6.2158
9571_at	YMR085W		Putative pseudogene	5.9695
10602_at	YKL050C		Similarity to YMR031c	5.9298
6694_at	YDL214C	PRR2	Strong similarity to putative protein kinase NPR1	5.9115
6221_at	YDR256C	CTA1	Catalase A	5.8344
8776_at	YNR064C		Similarity to R.capsulatus 1-chloroalkane halidohydrolase	5.7894
7781_at	YPL017C		Strong similarity to Lpd1p and other dihydrolipoamide dehydrogenases	5.7802
5220_at	YGL205W	POX1	Fatty-acyl coenzyme A oxidase	5.7535
11185_at	YJL153C	INO1	L-myo-inositol-1-phosphate synthase	5.748
3764_s_at	RDN37-1		35S ribosomal RNA	5.7449
8192_at	YOR348C	PUT4	Putative proline-specific permease	5.5983
2260_g_at	YGL205W	POX1	Fatty acid β-oxidation, acyl CoA oxidase activity	5.579
9756_at	YML089C		Questionable ORF	5.5214
6887_at	YCR010C	ADY2	Strong similarity to *Y. lipolytica* GPR1and Fun34	5.5037
7754_at	YPR002W	PDH1	Similarity to B.subtilis mmgE protein	5.4901
9510_at	YMR114C		Similarity to B. subtilis conserved hypothetical proteins yoqW and yoaM	5.4769
5416_at	SNR14		snRNA R14	5.4758
9063_at	YNL196C	SLZ1	Sporulation-specific protein with a leucine zipper motif, regulated by the transcription factor Ume6 and expressed early in meiosis	5.4619
9275_g_at	NC_001145		Chromosome XIII between NDI1 and YML119W	5.4135
7503_i_at	NC_001148		Several potential matches——not a good target probe	5.3878
10026_at	YLR311C		Weak similarity to *S.tarentolae* cryptogene protein G4	5.3443
7313_at	YBR045C	GIP1	Glc7-interacting protein.	5.3384
10154_at	YLR174W	IDP2	Cytosolic form of NADP-dependent isocitrate dehydrogenase	5.3254
4756_at	YGR236C	SPG1	Questionable ORF	5.305
2261_s_at	YGL205W	POX1	Fatty acid β-oxidation, acyl CoA oxidase activity	5.2987
9958_at	YLR377C	FBP1	Fructose-1,6-bisphosphatase	5.2692
7594_at	YPR151C	SUE1	Weak similarity to YPL159c	5.251

10795_at	YKL217W	JEN1	Carboxylic acid transporter protein homolog	5.2403
2259_at	YGL205W	POX1	Fatty acid β-oxidation, acyl CoA oxidase activity	5.2108
7403_at	YBL049W	MOH1	hypothetical protein	5.1576
5679_at	YER024W	YAT2	Similarity to carnitine O-acetyl-transferase Yat1p	5.1517
10478_at	YKR097W	PCK1	Phosphoenolpyruvate carboxylkinase	5.1145
7923_at	YPL147W	PXA1	Pxa1 and Pxa2 are subunits of a peroxisomal ATP-binding cassette transpor	5.1141
4388_at	YHR139C	SPS100	Sporulation-specific wall maturation protein	5.0933
7810_at	YPL033C		Weak similarity to YLR426w	5.0887
7254_at	YBR117C	TKL2	Transketolase, homologous to tkl1	5.085
10705_g_at	YKL124W	SSH4	Suppressor of SHR3; confers leflunomide resistance when overexpressed	5.0707
8881_at	YNL014W	HEF3	Translation elongation factor eEF3 homolog	5.0456
10027_at	YLR312C		Hypothetical protein	5.0439
10776_at	YKL187C		Strong similarity to hypothetical protein YLR413w	5.0154
4365_at	YHR160C	PEX18	YHR160C weak similarity to hypothetical protein YGR239c	5.0107
6765_at	NC_001135		Chr III between YCL049C and YCL048W	4.9988
6729_at	YDL223C	HBT1	Weak similarity to mucin	4.9932
11113_at	YJL089W	SIP4	Shows homology to DNA binding domain of Gal4p, has a leucine zipper motif and acidic region; lexA-Sip4p activates transcription	4.9621
9444_at	YMR174C	PAI3	Cytoplasmic inhibitor of proteinase Pep4p	4.9547
3850_at	YJRWDELTA20		Ty1 LTR	4.954
4561_s_at	SNR7-L		snRNA	4.9402
5627_at	YER096W	SHC1	Sporulation-specific homolog of csd4	4.932
6234_at	YDR223W		Similarity to Ifh1p	4.9079
6556_at	YDL085W	NDE2	Strong similarity to NADH dehydrogenase (ubiquinone)	4.8397
9668_at	YML042W	CAT2	Carnitine O-acetyltransferase, peroxisomal and mitochondrial	4.8313
11386_at	YAL062W	GDH3	NADP-linked glutamate dehydrogenase	4.817
9287_s_at	YMR322C	SNO4	Strong similarity to YPL280w, YOR391c and YDR533c	4.7818
7404_at	YBL048W		Hypothetical protein	4.6831
9274_at	NC_001145		Chromosome XIII between NDI1 and YML119W	4.6538
3878_s_at	TL(UAA)J		tRNA-Leu	4.6446
8504_at	YOR031W	CRS5	Metallothionein-like protein	4.6389
8939_at	YNL093W	YPT53	Rab5-like GTPase involved in vacuolar protein sorting and endocytosis	4.6127
4672_at	NC_001139		Chr VII near POX1	4.6107
4432_at	YHR096C	HXT5	Hexose transporter	4.4888
3545_i_at	YBLWDELTA1		Ty1 LTR	4.4554
4241_at	YIL160C	POT1	Peroxisomal 3-oxoacyl CoA thiolase	4.377
7409_at	YBL043W	ECM13	ExtraCellular Mutant	4.3717
6346_at	YDR111C		Strong similarity to alanine transaminase	4.3418
8228_at	YOR338W		Similarity to YAL034c	4.3346
7253_g_at	YBR116C		Questionable ORF	4.3188
9830_at	NC_001144		ChrXII near ACS2 and ribosomal proteins	4.3166
9026_at	YNL142W	MEP2	Ammonia transport protein	4.3021
7811_at	YPL079W	RPL21B	Ribosomal protein L21B	4.2806
9276_at	NC_001145		ChrXIII between NDI1 and YML119W	4.2775
9223_at	YMR175W-A		Near SIP18 (see Oshiro G, et al. (2002))	4.2721
9221_f_at	NC_001145		Chr XIII near YMR107W	4.2389
5612_at	YER084W		Questionable ORF	4.2363
10043_at	YLR284C	ECI1	Peroxisomal enoyl-CoA hydratase	4.2068
3255_at	YGRCDELTA20		Ty1 LTR	4.1922

9196_s_at	YNL335W		Similarity to M.verrucaria cyanamide hydratase, identical to hypothetical protein YFL061W	4.1854
11114_at	YJL088W	ARG3	Ornithine carbamoyltransferase	4.1805
3546_f_at	YBLWDELTA1		Ty1 LTR	4.1561
7714_at	YPR049C	CVT9	Similarity to Uso1p	4.1497
9549_at	YMR107W		Hypothetical protein	4.1346
9964_at	YLR340W	RPP0	60S ribosomal protein P0 (A0) (L10E)	4.1186
3858_s_at	TN(GUU)K		TN(GUU)K tRNA-Asn	4.1096
4923_at	YGR087C	PDC6	Third, minor isozyme of pyruvate decarboxylase	4.0937
10072_at	YLR267W	BOP2	Bypass of PAM1	4.087
9219_i_at	NC_001145		Chr XIII near YMR107W	4.0856
5528_at	YER179W	DMC1	Meiosis-specific protein related to RecA and Rad51	4.0835
6968_at	YBR230C	LSR1	U2 spliceosome RNA	4.0793
4900_at	YGR110W		Weak similarity to YLR099c and YDR125c	4.0688
5915_at	YDR536W	STL1	Sugar transporter-like protein	4.0658
4507_at	YHR033W		Probable γ-glutamyl kinase (Pro1)	4.0591
5755_at	YEL035C	UTR5	Protein of unknown function	4.0423
3243_at	TL(GAG)G		tRNA-Leu	4.0331
6980_at	NC_001134		ChrII between BAP2 and TAT1	4.0136

Table S4. List of the genes down-regulated 4-fold or lower at the T_{Dry} timepoint.

Probe	Gene	SDC	Annotation	Fold change
2837_s_at	YLR342W	FKS1	β-1,3 glucan biosynthesis, cell wall organization/biogenesis	-6.9885
2162_g_at	YGR234W	YHB1	Flavohemoglobin	-6.5145
4884_i_at	YGR138C	TPO2	Putative polyamine transport protein	-6.2211
9947_i_at	YLR367W	RPS22B	Ribosomal protein S22B (S24B) (rp50) (YS22)	-6.1321
7273_at	YBR092C	PHO3	Acid phosphatase, constitutive	-6.0281
4428_at	YHR092C	HXT4	High-affinity glucose transporter	-5.9432
6413_at	YDR044W	HEM13	Coproporphyrinogen III oxidase	-5.943
4491_at	YHR063C	PAN5	Pantothenate biosynthesis	-5.8044
2835_at	YLR342W	FKS1	β-1,3 glucan biosynthesis, cell wall organization/biogenesis	-5.7735
5750_at	YEL040W	UTR2	Weak similarity to Bacillus 1,3-1,4-beta-glucanase	-5.7656
8922_at	YNL066W	SUN4	Protein involved in the aging process	-5.7609
5571_at	YER131W	RPS26B	Ribosomal protein S26B	-5.6749
4813_at	YGR203W	YGR203W	Putative phosphotyrosine phosphatase	-5.6575
5667_at	YER055C	HIS1	ATP phosphoribosyltransferase	-5.6333
5005_at	YGL012W	ERG4	Sterol C-24 reductase	-5.5399
11355_at	YAL012W	CYS3	Cystathionine gamma-lyase	-5.5321
7694_at	YPR074C	TKL1	Transketolase 1	-5.5102
2838_s_at	YLR342W	FKS1	β-1,3 glucan biosynthesis, cell wall organization/biogenesis	-5.507
2163_s_at	YGR234W	YHB1	Flavohemoglobin	-5.5021
4478_at	YHR049W	FSH1	Similarity to S.pombe dihydrofolate reductase and YOR280c	-5.4671
8862_at	YNR014W	YNR014W	Weak similarity to hypothetical protein YMR206w	-5.4341
5178_at	YGL157W	YGL157W	Similarity to V.vinifera dihydroflavonol 4-reductase	-5.3728
7588_at	YPR145W	ASN1	Asparagine synthetase	-5.3467
9700_at	YML056C	IMD4	Strong similarity to IMP dehydrogenases	-5.3462
2839_s_at	YLR342W	FKS1	β-1,3 glucan biosynthesis, cell wall organization/biogenesis	-5.3233
5016_at	YGL001C	ERG26	Putative 3-beta-hydroxysteroid dehydrogenase	-5.3232
10658_at	YKL081W	TEF4	Translation elongation factor EF-1gamma	-5.2868
8246_s_at	YOR309C	YOR309C	Dubious ORF	-5.2326
6558_i_at	YDL083C	RPS16B	Ribosomal protein S16B (rp61R)	-5.1873
10800_at	YKL212W	SAC1	Phosphoinositide phosphatase	-5.1643
6560_at	YDL082W	RPL13A	Ribosomal protein L13A	-5.1556
7190_i_at	YBR189W	RPS9B	Ribosomal protein S9B (S13) (rp21) (YS11)	-5.0773
6131_at	YDR345C	HXT3	High-affinity glucose transporter	-4.9943
7413_at	YBL039C	URA7	CTP synthase, highly homologus to URA8 CTP synthase	-4.9041
4754_at	YGR234W	YHB1	Flavohemoglobin	-4.9026
11203_i_at	YJL177W	RPL17B	Ribosomal protein L17B (L20B) (YL17)	-4.8839
2280_s_at	YEL022W	GEA2	ARF guanyl-nucleotide exchange factor activity, ER to Golgi transport, intra-Golgi transport	-4.8646
8548_at	YOL014W	YOL014W	Hypothetical protein	-4.8451
7103_at	YBR238C	YBR238C	Similar to RMD9 (required for meiotic nuclear division)	-4.8276
10700_at	YKL128C	PMU1	Phospo-mutase homolog	-4.7959
2836_g_at	YLR342W	FKS1	β-1,3 glucan biosynthesis, cell wall organization/biogenesis	-4.7956
5698_at	YER043C	SAH1	Putative S-adenosyl-L-homocysteine hydrolase	-4.7395
5076_f_at	YGL076C	RPL7A	Ribosomal protein L7A (L6A) (rp11) (YL8)	-4.6974
10160_at	YLR180W	SAM1	S-adenosylmethionine synthetase	-4.6871
8355_at	YOR198C	BFR1	Implicated in secretion and nuclear segregation, associates with Scp160p	-4.6578
5260_at	YGL253W	HXK2	Hexokinase II (PII) (also called Hexokinase B)	-4.657
9699_at	YML056C	IMD4	Strong similarity to IMP dehydrogenases	-4.6511
8247_at	YOR310C	NOP58	nucleolar protein involved in the pre-rRNA processing steps that lead to formation of 18 S rRNA; interacts with Nop1p	-4.6423
7461_at	YBL081W	YBL081W	hypothetical protein, asparagine rich	-4.5991
9761_at	YML124C	TUB3	alpha-tubulin	-4.5927
6612_at	YDL119C	YDL119C	transporter activity, mitochondrial inner membrane	-4.5837

6665_at	YDL198C	YHM1	High copy suppressor of abf2 lacking the HMG1-like mitochondrial HM protein; putative mitochondrial carrier protein	-4.5683
8577_at	YOL030W	GAS5	Strong similarity to glycoprotein Gas1p	-4.5443
5664_at	YER052C	HOM3	Aspartate kinase, first step in Met and Thr biosynthesis	-4.5217
8022_at	YPL273W	SAM4	AdoMet-homocysteine methyltransferase	-4.5148
9661_at	YML008C	ERG6	S-adenoslymethionine: delta 24-methyltransferase, ergosterol biosynthesis	-4.5146
4493_at	YHR020W	YHR020W	proline-tRNA ligase activity, required for cell viability	-4.5113
6712_at	YDL241W	YDL241W	hypothetical protein	-4.5036
9312_at	YMR305C	SCW10	Souble cell wall protein with glycosidase activity	-4.502
4538_at	YHR019C	DED81	Asparaginyl-tRNA synthetase	-4.4954
5310_at	YFR055W	YFR055W	Strong similarity to beta-cystathionases	-4.4945
10132_at	YLR197W	SIK1	Part of small (ribosomal) subunit (SSU) processosome	-4.4879
7993_at	YPL256C	CLN2	G(sub)1 cyclin, cyclin-dependent protein kinase, re-entry into mitotic cell cycle after pheromone arrest, regulation of CDK activity	-4.4716
8269_f_at	YOR293W	RPS10A	Ribosomal protein S10A	-4.4628
4851_i_at	YGR151C	YGR151C	Questionable ORF	-4.4563
8646_at	YOL097C	WRS1	Cytoplasmic tryptophanyl-tRNA synthetase	-4.4055
10029_at	YLR314C	CDC3	Phosphatidylinositol binding, structural constituent of cytoskeleton, a septin involved in bud growth	-4.3959
6869_at	YCR034W	FEN1	Fatty acid elongase activity, and is also involved in synthesis of 1,3-β-glucan, a component of the cell wall	-4.3787
5467_f_at	NC_001137		Chr V between POL5 and RPL12A	-4.3778
4368_at	YHR163W	SOL3	Shows similarity to glucose-6-phosphate dehydrogenase non-catalytic domains; homologous to Sol2p and Sol1p, tRNA processing	-4.3762
11122_at	YJL080C	SCP160	mRNA binding protein, associates with polyribosomes	-4.3739
9691_i_at	YML063W	RPS1B	Ribosomal protein S1B (rp10B)	-4.3606
9704_at	YML052W	SUR7	Localized at cortical patches, interacts with cell wall, affects sphingolipid metabolism	-4.3571
8801_at	YNR043W	MVD1	Mevalonate pyrophosphate decarboxylase, ergosterol/isoprenoid metabolism	-4.3562
7262_at	YBR084W	MIS1	Mitochondrial C1-tetrahydroflate synthase; related to formylation of the initiator tRNA	-4.3341
5223_at	YGL202W	ARO8	Aromatic amino acid aminotransferase	-4.3301
11237_at	YJL189W	RPL39	Ribosomal protein L39 (L46) (YL40)	-4.3282
7960_i_at	YPL198W	RPL7B	Ribosomal protein L7B (L6B) (rp11) (YL8)	-4.3281
9397_at	YMR215W	GAS3	Similarity to GAS1 protein	-4.3227
5556_at	YER163C	YER163C	Hypothetical protein, uncharacterized ORF	-4.3048
4868_at	YGR123C	PPT1	Serine/threonine phosphatase, highest in early log phase (ie., excess nutrients)	-4.3021
4818_at	YGR208W	SER2	Phosphoserine phosphatase	-4.2925
5396_at	YFL034C-A	RPL22B	Ribosomal protein L22B (L1c) (rp4) (YL31)	-4.2915
10159_at	YLR179C	YLR179C	Phosphatidylethanolamine-binding motif	-4.2599
8235_at	YOR301W	RAX1	Verified ORF related to bud site selection	-4.2594
8729_at	NC_001146		Chr XIV, may be part of snR40 (small nucleolar RNA)	-4.232
4343_at	YHR183W	GND1	Phosphogluconate Dehydrogenase (Decarboxylating)	-4.2265
4256_at	YIL145C	PAN6	Pantothenate synthetase	-4.2258
5550_at	YER156C	YER156C	Hypothetical protein	-4.2194
8698_at	YOL136C	PFK27	6-phosphofructo-2-kinase, regulation of glycolysis	-4.216
4769_at	YGR249W	MGA1	Shows similarity to heat shock transcription factor, related to filamentous growth	-4.2119
2182_s_at	YGL195W	GCN1	Regulation of translation elongation	-4.2079
7114_at	YBR249C	ARO4	3-deoxy-D-arabino-heptulosonate 7-phosphate (DAHP) synthase isoenzyme	-4.2032

5100_at	YGL097W	SRM1	Signal transducer activity, rRNA-nucleus export, ribosome nucleus export	-4.1976
9185_at	YNL300W	TOS6	Putative glycosylphosphatidylinositol-attached protein	-4.1857
5465_f_at	NC_001137		Chr V between POL5 and RPL12A	-4.1813
8244_i_at	YOR309C	YOR309C	Questionable ORF	-4.1742
10976_at	YJR047C	ANB1	Anaerobically expressed form of translation initiation factor eIF-5A	-4.1683
10247_at	YLR083C	EMP70	Integral membrane protein; putative transporter	-4.1671
6438_at	YDR023W	SES1	Seryl-tRNA synthetase	-4.1661
2841_s_at	YLR342W	FKS1	β-1,3 glucan biosynthesis, cell wall organization/biogenesis	-4.1565
5216_at	YGL209W	MIG2	RNA polymerase II transcription factor activity	-4.1491
10556_i_at	YKL006W	RPL14A	Ribosomal protein L14A	-4.1425
7027_at	NC_001134		Chr II between YBR161W and TOS1	-4.1401
9953_at	YLR372W	SUR4	Conversion of 24-carbon fatty acids to 26-carbon species	-4.1236
7693_at	YPR073C	LTP1	Phosphotyrosine phosphatase of unknown function	-4.1219
6493_at	YDL014W	NOP1	Part of small (ribosomal) subunit (SSU) processosome, associates with Nop58p, methyltransferase activity	-4.1119
8048_at	NC_001147		Chr XV between MSC6 and GDS1	-4.109
2589_g_at	YOR341W	RPA190	Subunit of DNA polymerase I	-4.1052
6174_at	YDR300C	PRO1	γ-Glutamyl kinase	-4.1002
4499_at	YHR025W	THR1	Homoserine kinase	-4.0993
6513_at	YDL039C	PRM7	Plasma membrane fusion, expressed during mating	-4.0978
9484_at	YMR131C	RRB1	Regulation of ribosome biosynthesis	-4.0937
9497_i_at	YMR143W	RPS16A	Ribosomal protein S16A (rp61R)	-4.091
10473_i_at	YKR094C	RPL40B	YKR094C Ribosomal protein L40B	-4.0884
10576_at	YKR013W	PRY2	Unknown function, regulated by Ste12p, homology to the plant PR-1 class of pathogen related proteins	-4.0752
9399_at	YMR217W	GUA1	GMP synthase, purine nucleotide biosynthesis	-4.0575
7257_at	YBR121C	GRS1	Glycyl-tRNA synthase	-4.0492
6452_at	YDR037W	KRS1	Lysyl-tRNA synthetase	-4.0343
4941_at	YGR060W	ERG25	C-4 sterol methyl oxidase	-4.0292
7855_f_at	YPL081W	RPS9A	Ribosomal protein S9A (S13) (rp21) (YS11)	-4.0262
7741_at	YPR033C	HTS1	Cytoplasmic and mitochondrial histidine tRNA synthetases	-4.0192
2183_s_at	YGL195W	GCN1	Regulation of translation elongation	-4.0135
7338_at	YBR025C	YBR025C	Unknown function, regulated by Skn7p	-4.0027

Table S5. Four-fold and higher upregulated genes within biological, cellular and molecular GO categories in comparison with transcription level at T_1 (also see Fig. S1).

Gene	Description	Function	Process	Component
SIP18	salt-induced	phospholipid binding	desiccation, osmotic stress	soluble fraction
POX1	fatty-acyl CoA oxidase	acyl CoA oxidase	fatty acid β-oxidation	peroxisomal
POT1	3-oxoacyl CoA thiolase	Ac CoA C-acyltransferase	fatty acid β-oxidation	peroxisomal
IDP3	NADP-dependent isocitrate dehydrogenase	isocitrate dehydrogenase NADP+	fatty acid β-oxidation NADPH regeneration	peroxisomal cytoplasm
FOX2	multifunctional b-oxidation protein	3-hydroxyacyl-CoA dehydrogenase; enoyl-CoA hydratase	fatty acid β-oxidation	peroxisomal
DCI1	Δ3,5 -Δ2,4 -dienoyl-CoA isomerase	dodecenoyl-CoA Δ-isomerase	fatty acid β-oxidation	peroxisomal isomerase
GRE1	osmotic stress induced	unknown	desiccation, stress	cytoplasm
CIT3	Mitochondrial isoform of citrate synthase	citrate synthase	citrate, propionate metabolism; TCA cycle	mitochondrial matrix
PDH1	prpD homologue;propionate catabolism in *E. coli*	unknown	propionate metabolism	unknown
SSA3	70 kDa heat shock protein family	heat shock protein	SRP-dependent, co-translational membrane targeting, translocation; protein folding; protein-mitochondrial targeting; stress	cytoplasm
YAT2	homology with known carnitine acetyltransferase	carnitine O-Ac transferase	alcohol/carnitine metabolism	unknown
FBP1	fructose-1,6-bisphosphatase	fructose-bisphosphatase	gluconeogenesis	cytosol
YAT1	carnitine acetyltransferase, outer mitochondrial	carnitine O-Ac transferase	alcohol/carnitine metabolism	mitochondrion
SFC1	succinate-fumarate carrier	succinate/fumarate antiporter	succinate/fumarate transport	mitochondrion inner membrane
CAT2	carnitine O-acetyltransferase peroxisomal/mitochondrial	carnitine O-acetyltransferase	carnitine metabolism	mitochondrion peroxisomal
MLS1	carbon-catabolite sensitive malate synthase	malate synthase	glyoxylate cycle	cytoplasm peroxisomal
GIP1	Developmentally-regulated protein phosphatase 1, Glc7	protein phosphatase 1 binding	spore wall assembly *sensu Saccharomyces*	prospore membrane,

	interacting protein required for spore formation			protein phosphatase type 1 complex
PXA1	subunits of a peroxisomal ATP-binding cassette transporter necessary for transport of long-chain fatty acids into peroxisomes	ATP-binding cassette ABC transporter	fatty acid transport	integral peroxisomal membrane
PEX18	peroxin	protein binding	protein-peroxisome targeting	cytosol peroxisomal
SPS19	late sporulation specific gene which may function during spore wall formation	2,4-dienoyl-CoA reductase NADPH	fatty acid catabolism sporulation *sensu Saccharomyces*	peroxisomal
PXA2	homolog of the human adrenoleukodystrophy transporter; heterodimer with Pxa1p of two half ATP-binding cassette transporters in the peroxisome membrane	ATP-binding cassette ABC transporter	fatty acid transport	integral peroxisomal membrane
PEX21	peroxin	protein binding	protein-peroxisome targeting	cytosol peroxisomal
ECI1	enoyl-CoA isomerase	dodecenoyl-CoA Δ-isomerase	fatty acid β-oxidation	peroxisomal

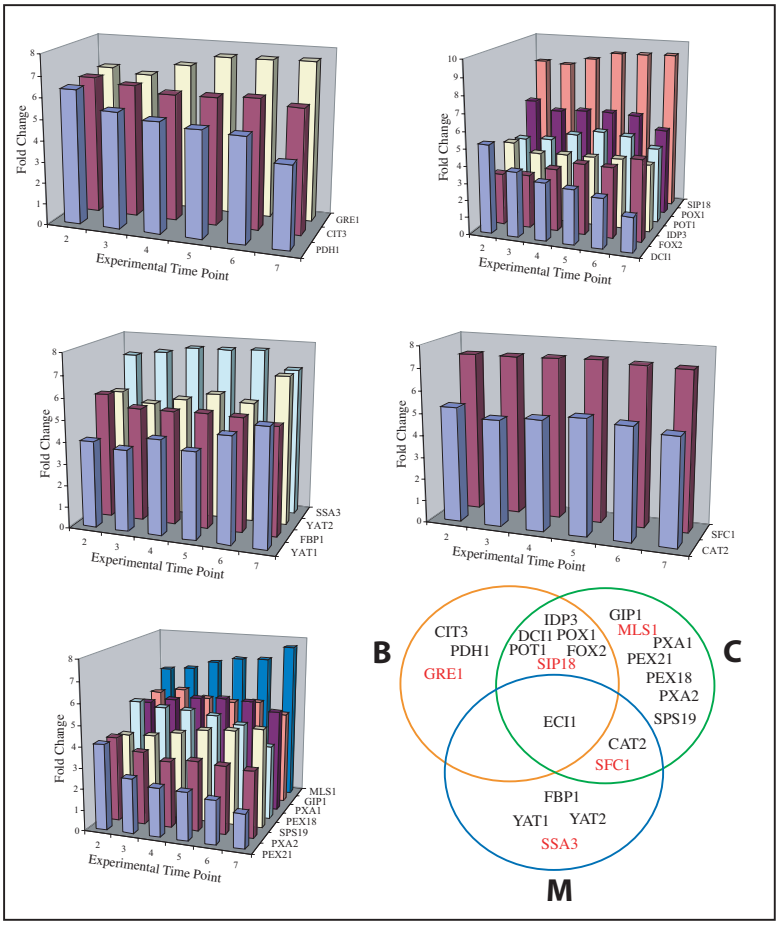

Fig. S1. Four-fold and higher up regulated genes within biological, cellular and molecular GO categories in comparison with transcription level at Timepoint 1 (also see Table S5).

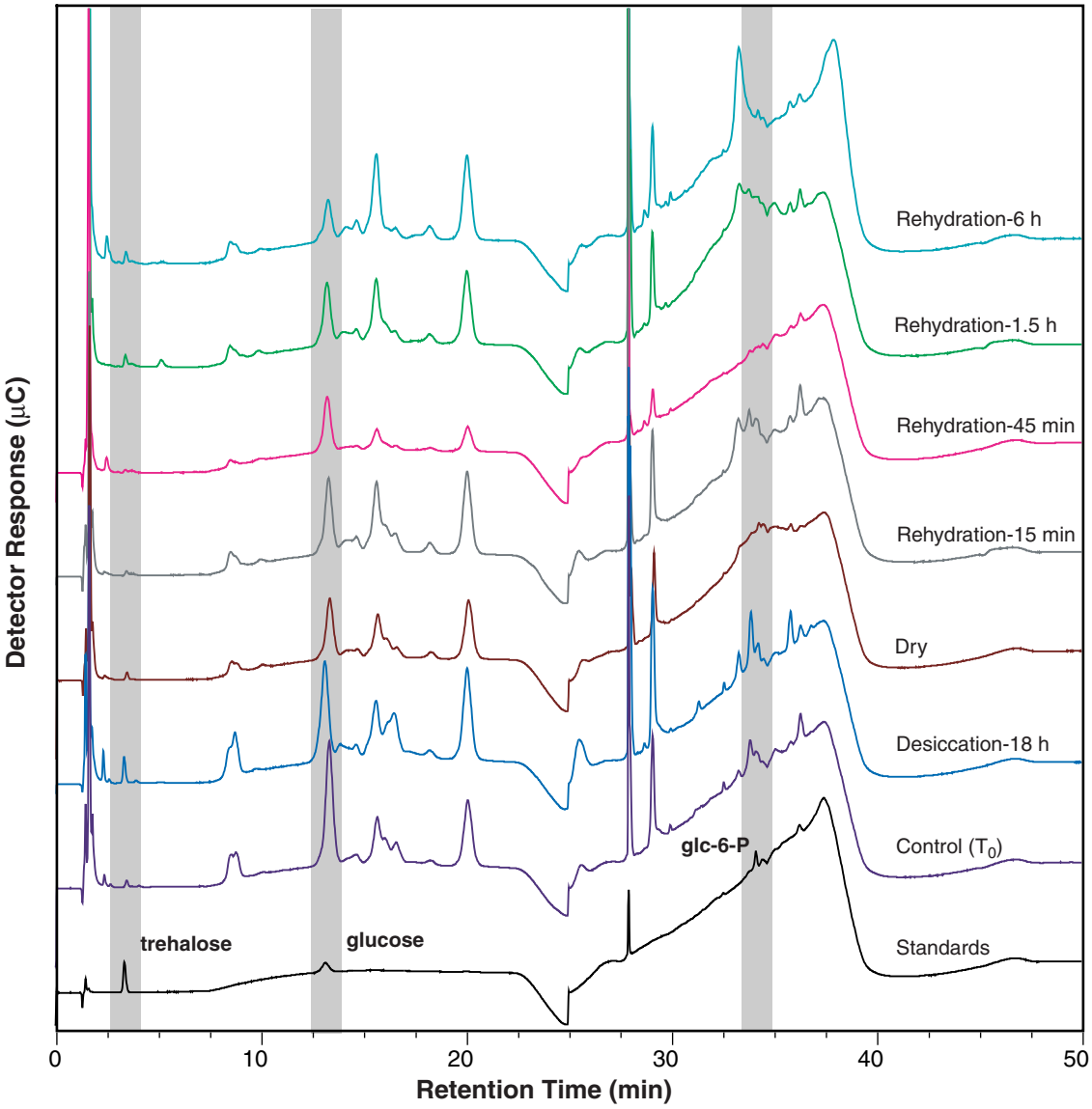

Fig. S2. High performance anion-exchange chromatographic separation of the yeast cell extracts (see Supplemental Materials and Methods for sample preparation and analysis). Elution times of trehalose, glucose and glucose 6-phosphate are indicated. Quantities present were below those required for accurate determination of concentration. However, amounts injected are on an equivalent cell mass basis. There is clearly a slight increase in the trehalose levels during the drying phase of the experiment, and detectable glucose is present at all time points.

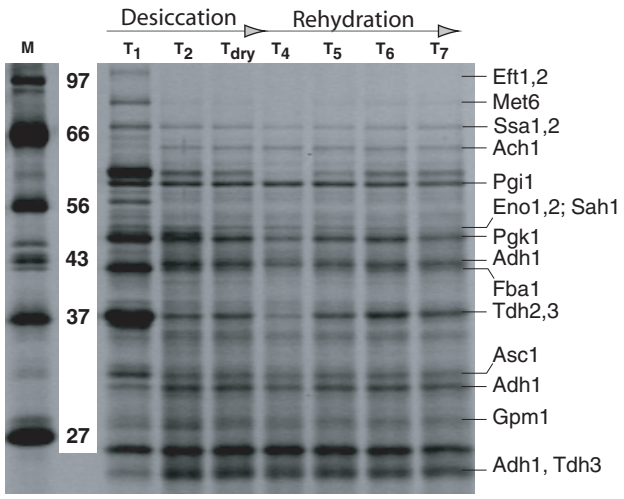

Fig. S3. Sypro-Ruby stained SDS-PAGE gel (12%) of the soluble protein fractions of yeast obtained during desiccation and rehydration. The major proteins identified by in-gel tryptic digestion/LC-tandem mass spectrometry are indicated on the right.

Total soluble proteins from a portion of the yeast cells obtained at each time point were analysed by one-dimensional SDS-PAGE gel electrophoresis at equivalent protein loading levels. As cells underwent the initial phases of desiccation there was an overall decrease in the intensity of bands in the 25-100 kDa range, with the least intense lane being that of the first rehydration time point. Several stained bands were then picked manually and analyzed as tryptic digests by nanoflow LC-ion trap mass spectrometry. The gluconeogenesis proteins Pgi1, Pgk1 and Tdh2,3 were the major proteins present in the more intensely staining bands throughout the treatment regime. The appearance of multiple forms of Adh1 and Tdh2,3 was also observed. Their presence at multiple locations on the gel could be due to the unavoidable inclusion of non-viable cells in the cell pellet used for protein extraction.

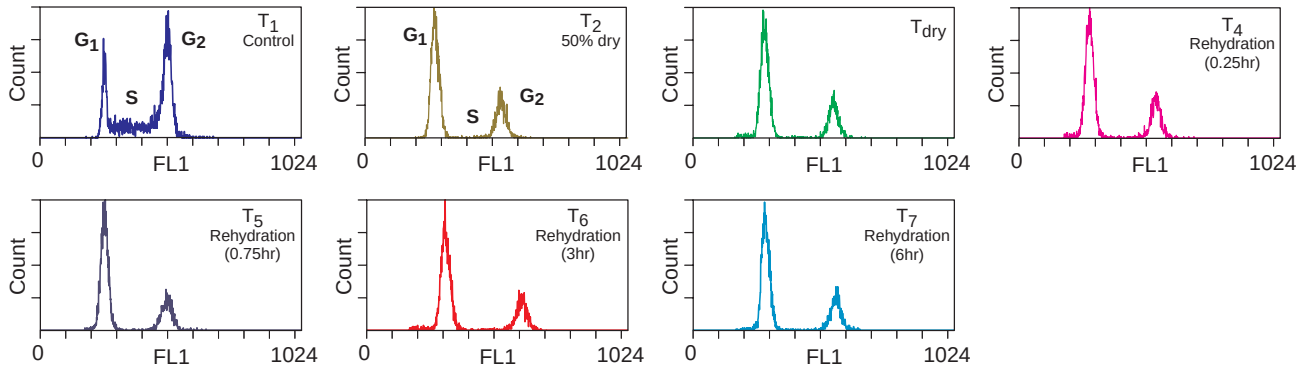

Fig. S4. Results of the FACS Analyses (SYTOX staining). Only the G1 and G2 phases were detected immediately after rehydration of the dried sample. These cells presumably had adapted to desiccation, as there was little to no loss of viability during 72h of storage, and following addition of fresh medium and subsequent incubation. It took approximately 44h for cells to resume growth and for the population to acquire a normal FACS profile in 1/20 YPD, at 25°C, (data not shown). In full strength YPD, at 30°C, FACS analysis first detected a "normal" profile at approximately 13h (data not shown).

Fig. S5. Redescriptions R1—R12. See page S27 for the Figure Legend.

Redescription R1

Heat Shock, 20 min ≥ 1 AND DBY7286, 0.3 mM H_2O_2, 20 min ≤ -1 ⟷
Increased expression with respect to T_{dry} till T_5 and then a leveling off.

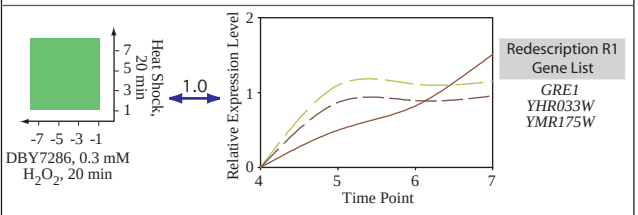

Redescription R2

1M sorbitol, 30 min ≥ 2 AND NOT 29 °C, 1M sorbitol to 33 °C, 1M sorbitol, 30 min ≥ 1 ⟷ Increased expression with respect to T_{dry} from T_5 onwards.

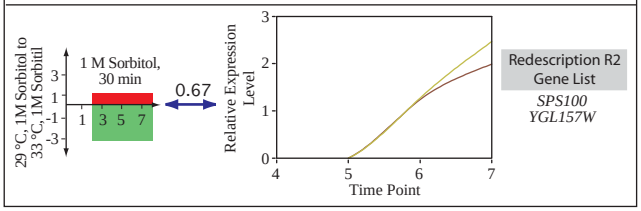

Redescription R3

0.32 mM H_2O_2, 30 min ≥ 2 AND NOT 0.32 mM H_2O_2, 50 min ≥ 2 ⟷
T_7 vs T_1 ≤ 4 AND T_7 vs T_{dry} ≥ 4

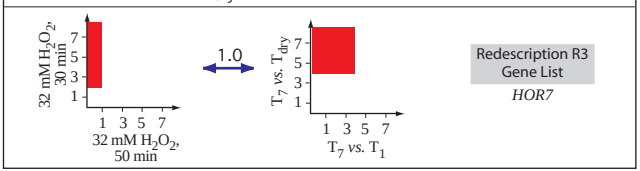

Redescription R4

T_2 vs T_1 ≥ -2 AND T_7 vs T_{dry} ≥ 1 AND T_7 vs T_{dry} ≤ 3
⟷ 1M sorbitol, 15 min ≤ -2.
⟷ DBYmsn2/4, 0.32 mM H_2O_2, 20 min ≤ -2
⟷ Heat Shock, 30 min ≤ -3
⟷ Heat Shock, 10 min ≤ -4
⟷ Heat Shock, 20 min ≤ -4
⟷ Heat Shock, 15 min ≤ -5

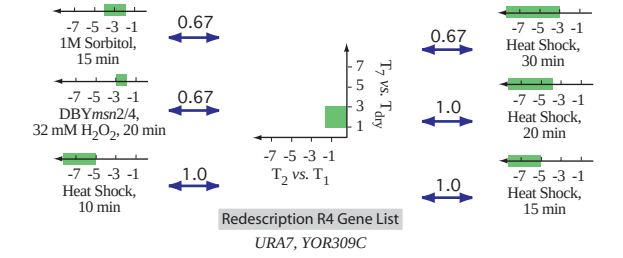

Redescription R5

Heat Shock, 30 min ≤ -1 ⟷ T_2 vs T_1 ≥ -5 AND NOT T_2 vs T_1 ≥ -1

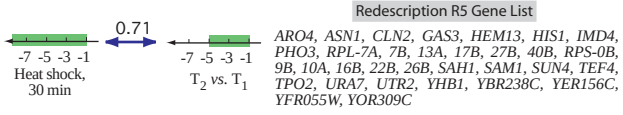

Redescription R6

Soluble fraction AND NOT Nucleus ⟷ T_5 vs T_1 ≥ 6 AND T_5 vs Tdry ≤ 1

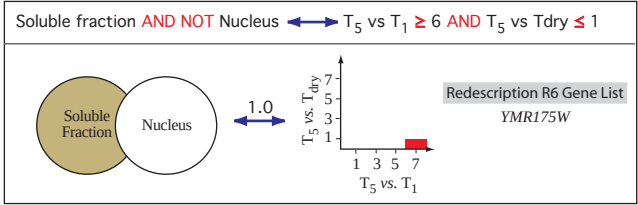

Redescription R7

Heat Shock, 10 min ≤ -5 AND Heat Shock, 15 min ≤ -5 OR NOT Heat Shock 10 min ≤ -5 AND Heat Shock 20 min ≤ -1 ⟷ Downward trend initially and then an upward trend

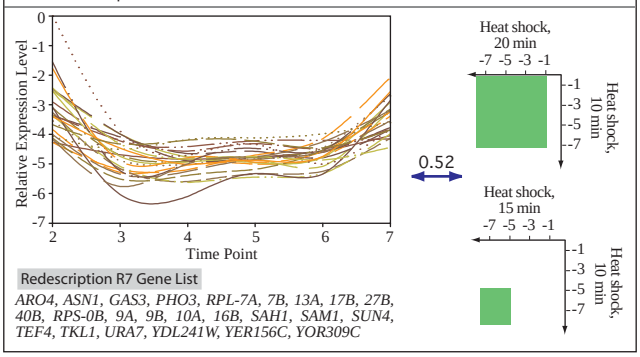

Redescription R8

T_4 vs T_1 ≥ 5 ⟷ YPD, 1 day ≥ 2 AND NOT 0.32 mM H_2O_2, 40 min ≥ 1
T_5 vs T_1 ≥ 5 ⟷ YPD, 1 day ≥ 2 AND NOT 0.32 mM H_2O_2, 40 min ≥ 1

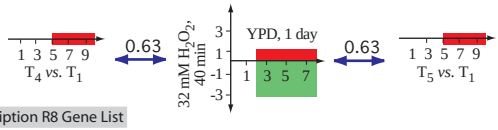

ADY2, CAT2, CIT3, CTA1, FBP1, FDH2, GRE1, HBT1, HEF3, HXT5, IDP2, INO1, JEN1, MLS1, NDE2, PCK1, PDH1, POX1, PUT4, PXA1, SIP18, SFC1, SLZ1, SPG1, SPS100, SSA3, SUE1, TKL2, YAT2, YJL045W, YKL050C, YKL107W, YKL187C, YLR312C, YMR085W, YMR107W, YMR114C, YMR118C, YPL201C

Redescription R9

T_{dry} vs T_1 ≥ -6 AND NOT Dry Active Yeast ≥ 0 ⟷ Heat Shock, 10 min ≤ -1
⟷ Heat Shock, 15 min ≤ -1
⟷ Heat Shock, 20 min ≤ -1
⟷ Heat Shock, 30 min ≤ -1

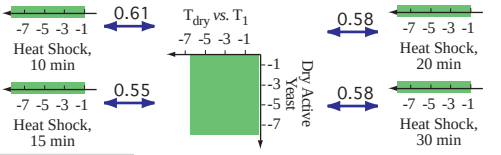

ARO4, HIS1, IMD4, RPL-7A, 7B, 13A, 17B, 27B, 40B, RPS-0B, 9B, SAC1, SAH1, SUN4, TEF4, TKL1, URA7, UTR2, YHM1, YER156C, YOR309C

Redescription R10

T_{dry} vs T_1 ≥ 4 AND Dry Active Yeast ≥ 6 ⟷ Heat Shock, 15 min ≥ 2
⟷ Heat Shock, 20 min ≥ 2
⟷ Heat Shock, 30 min ≥ 2

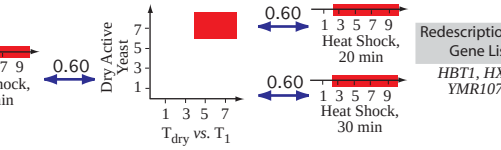

Redescription R11

T_2 vs T_1 ≥ 7 ⟷ Histone Depletion, 4h ≥ 5 AND NOT Histone Depletion, 4h ≥ 6

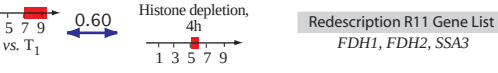

Redescription R12

T_7 vs T_1 ≤ -5 ⟷ Histone Depletion, 0.5h ≥ 3 AND Histone Depletion, 4h ≤ 2

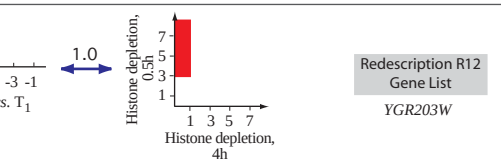

Fig. S5. Redescriptions R1 through R12. The top panel of each redescription describes the redescription in a text format. The bottom panel shows the redescription in graphical format. The Jaccard coefficient for each redescription is shown over the redescription arrow. Also included in the bottom panel is the gene list obtained from the redescription. Limiters are in place for fold changes so that they do not pass through a fold change of zero. Thus when a fold change states greater than -2, a range from -2 to 0 is meant. If a region defined in the graphical format extends to the end of the axis, it indicates that genes above the highest value listed on the axis will still be included (*ie.*, there is no upper limit of the fold change value).

Redescriptions R1—R8 compare our BY4743 data with that published by Gasch AP, Spellman PT, Kao CM, Carmel-Harel O, Eisen MB, Storz G, Botstein D, and Brown PO [*Genomic expression programs in the response of yeast cells to environmental changes, Mol. Biol. Cell* **11** (2000) 4241-4257]. Notice that some redescriptions such as R4 are multi-way and provide more than two ways to describe a given set of genes. Also, some redescriptions involve only one gene (R3, R6), while some others involve tens of genes (R5, R7, R8).

Redescriptions R9 and R10 combine our BY4743 data with that we obtained from a commercial dry active yeast and the heat shock experiments of Gasch *et al*.

Redescriptions R11 and R12 compare our BY4743 data with that obtained from the histone depletion data published by Wyrick JJ, Holstege FC, Jennings EG, Causton HC, Shore D, Grunstein M, Lander ES, and Young RA [*Chromosomal landscape of nucleosome-dependent gene expression and silencing in yeast. Nature* **402** (1999) 418-421].